



Influence of the steel plate on the friction behavior of automotive wet disk clutches

P. Strobl¹ · T. Schneider¹ · K. Voelkel¹ · K. Stahl¹

Received: 31 January 2023 / Accepted: 27 April 2023 / Published online: 30 May 2023
© The Author(s) 2023

Abstract

Friction behavior is the key parameter for the design of automotive wet disk clutches. On the one hand, the Coefficient of Friction (CoF) level should be high to transmit torque efficiently. On the other hand, the clutch requires a positive slope of the CoF over sliding speed for good controllability, high comfort, and a low tendency to shudder. Clutches used in automatic or dual-clutch transmissions mostly use organic friction lining. These friction systems tend to have low CoF at low sliding speeds due to their high requirements regarding shifting comfort. Nevertheless, they show high values of CoF at high sliding speeds.

This study investigates the influence of different steel plate finishes on friction behavior in different application-relevant operation modes such as brake shift, unsteady slip, and micro slip. Each of these operation modes requires an accurate CoF measurement at different sliding speed ranges. Therefore, we use different test rig setups. We characterize the steel plates by their areal surface topography measured with an optical system using focus variation. We discuss differences in the friction behavior of the corresponding tribological systems at different operating conditions.

Results show an influence of the steel plate surface finish on the CoF level. Therefore, the surface finish of the steel plate influences the functional behavior of wet disk clutches and engineers should consider the surface finish in the early design phase. We discuss the correlation between commonly used surface parameters and friction parameters.

Einfluss der Stahllamellenendbearbeitung auf das Reibungsverhalten von nasslaufenden Lamellenkupplungen in Kraftfahrzeugen

Zusammenfassung

Das Reibungsverhalten ist der entscheidende Parameter für die Entwicklung nasslaufender Lamellenkupplungen. Dabei soll die Reibungszahl zum einen möglichst hoch sein, um Drehmoment zuverlässig zu übertragen, zum anderen benötigt die Kupplung für eine gute Regelbarkeit, hohen Komfort und eine geringe Reibschwingneigung einen positiven Gradienten der Reibungszahl über der Gleitgeschwindigkeit. In Automat- und Doppelkupplungsgetrieben werden meist Kupplungen mit organischen Reibbelägen eingesetzt. Diese Reibsysteme neigen aufgrund ihrer hohen Anforderungen bzgl. Schaltkomfort zu sehr niedrigen Reibungszahlen bei kleinsten Gleitgeschwindigkeiten. Dennoch weisen sie in der Regel hohe Reibungszahlwert bei hohen Gleitgeschwindigkeiten auf.

✉ P. Strobl
patrick.strobl@tum.de

T. Schneider
thomas.schneider@tum.de

K. Voelkel
katharina.voelkel@tum.de

K. Stahl
karsten.stahl@tum.de

¹ School of Engineering and Design, Department of Mechanical Engineering, Gear Research Center (FZG), Technical University of Munich, Boltzmannstraße 15, 85748 Garching near Munich, Germany

Diese Publikation beschäftigt sich mit dem Einfluss von gängigen Stahllamellenendbearbeitungen auf das Reibungsverhalten in unterschiedlichen Betriebsmodi wie Bremsschaltungen, instationären Schlupf und Mikroschlupf. Diese Betriebsmodi erfordern jeweils eine hochgenaue Messung der Reibungszahl in den unterschiedlichen Gleitgeschwindigkeitsbereichen, weshalb unterschiedliche Prüfumgebungen genutzt werden. Die Stahllamellen werden anhand ihrer flächenhaften Oberflächentopografie charakterisiert. Diese wird mit einem optischen Messsystem mittels des Prinzips der Fokusvariation bestimmt. Es werden Unterschiede im Reibungsverhalten der entsprechenden Reibsysteme bei diversen Betriebsbedingungen diskutiert.

Die Ergebnisse weisen auf einen Einfluss der Stahllamellenendbearbeitung auf das Reibungszahlniveau hin. Aus diesem Grund muss die Endbearbeitung der Stahllamellen und dessen Einfluss auf das Funktionsverhalten in der frühen Entwicklungsphase nasslaufender Kupplungssysteme berücksichtigt werden. Es wird der Zusammenhang zwischen üblichen Oberflächen- und Reibungszahlkennwerten untersucht.

1 Introduction

Wet disk clutches and brakes provide differential speed shifting. In automotive drivelines, they are key components of dual-clutch and automatic transmissions, as well as of limited slip differentials and other applications. Here, the focus is on the friction behavior of wet disk clutches used in dual-clutch and automatic transmissions. In these applications, high comfort and fast shifting are the main requirements for the machine element. Therefore, the clutch must guarantee a high Coefficient of Friction (CoF) with a positive slope of the CoF over sliding speed to prevent self-excited vibrations, also known as shudder. This results in low CoF at low sliding speeds and, therefore, a low static torque capacity. In dual-clutch and automatic transmissions, organic friction materials are often used in combination with lubricants with appropriate additives to meet these conditions.

Thus, it is only possible to determine the friction behavior of a friction system by experimental investigation due to the high number of influencing parameters and their complex interactions. Therefore, there is ongoing research on these influences and their interactions.

In this context, mechanical and thermal loads, as well as the operation mode, can have a substantial impact on the frictional behavior. As mentioned above, the CoF should have a positive slope over sliding speed. This results in a strong influence of the sliding speed on friction behavior (e.g., [1–7]). Besides this, the specific surface pressure p may also affect the friction behavior (e.g., [5, 6]). Many investigations mention the strong influence of the clutch temperature on the frictional properties (e.g., [8–14]). To measure this influence, the oil injection temperature is often varied (e.g., [12, 14]) because the clutch temperature itself is hard to control directly during the run. Due to its importance, there are several ways to determine the temperatures of the clutch using simulations (e.g., [15–18]). For this reason, there are empirical-based models (e.g., [19–21]) to describe the influence of the mechanical and thermal loads on the friction behavior of wet disk clutches.

Lloyd et al. [22] discuss the static and dynamic friction behavior. They show differences between different measurement methods (steady-state, break-away, and endpoint friction) for measuring static friction torque and varying the clutch temperature due to different dwell times. Therefore, the measurement method itself shows an influence on the measured friction behavior. Besides the operation mode, even a variation of the time of standstill after shifting can also affect the friction behavior of wet disk clutches [23]. Therefore, methods for good characterization of the friction behavior are needed. Meingassner [13], Meingassner et al. [14, 24] and Voelkel et al. [12] develop a methodology to investigate the friction coefficient behavior from very low to comparatively high sliding speeds and shows a good transferability of the results between each other.

Fluctuations of the frictional behavior due to tolerances are often described in the literature (e.g., [13, 25, 26]). These must be considered in the evaluation methods, especially at low sliding speeds. Their influence could be overlooked due to low sliding paths.

The lubricant crucially influences the friction behavior of wet disk clutches. Previous investigations show, for example, influences of base oil [9], additives [3, 4, 8, 27], or oil aging [28] on the friction behavior.

Besides those influences, the used friction material also has a strong influence on the friction behavior. Ito et al. [1] state that the porosity of the organic friction materials affects the oil film pressure. However, the Young's modulus of the friction material may also have an impact on friction behavior, according to Katsukawa [29]. Even the microstructure of paper-based friction material can affect the frictional properties of a friction system [30].

In addition to the friction lining and the lubricant, the influence of the steel friction surface on the friction behavior of wet disk clutches is investigated in the literature. Voelkel [31] and Voelkel et al. [32] investigate the influence of different surface finishes on the friction behavior and its change during the run-in. Besides the influence of a mechanical surface finish, the nitriding of the steel plates can also improve the durability and friction behavior of the

clutch [33]. Furthermore, the manufacturing parameters of the surface finish itself can also affect the friction behavior. Investigations of steel plates finished with a face traverse grinding process show this influence with different lubricants [2, 7].

The roughness of both, friction lining and steel plate, influences the friction behavior of the wet disk clutches. Therefore, a suitable characterization of the surface topography is needed. Many researchers [7, 33] characterize the surface topography of friction surfaces using the profile method according to DIN EN ISO 21920-2 [34]. In recent years, the application of three-dimensional or areal measurement of friction surfaces has become more common (e.g., [31, 32, 35, 36]). The areal characterization of rough surfaces is standardized according to DIN EN ISO 25178-2 [37]. Some investigations use areal parameters for the characterization of steel and friction lining plates (e.g. [31, 35, 36]).

In summary, there is a gap in the research on the influence of steel plate finish in connection with standard areal surface parameters on the frictional behavior at low sliding speeds. In this publication, we therefore present the results of investigations with wet disk clutches with organic friction lining in combination with three near-application finishes of steel plates. We characterize the surface topography of the steel plate with areal surface parameters determined by the principle of focus variation. Then, the friction behavior of the friction systems with different steel plate finishings in three application-relevant operation modes (brake shifts, forced unsteady slip, and micro slip) is discussed. After that, we investigate linear relations between CoF and surface topography parameters. The results are discussed, and key statements are summarized.

2 Method

We investigate the friction behavior of a distinguished combination of friction lining and lubricant with different steel plate finishes in various operation modes using two component test rigs. Additionally, we measure the surface topography of the steel plates after the run-in. First, the tested parts are introduced. Fig. 1 shows an internally toothed friction plate with organic friction lining from a dual-clutch application and an externally toothed steel plate. For the investigations, each clutch consists of four steel plates and three friction plates leading to a total number of six friction surfaces ($z=6$). The plates are mounted alternately in the corresponding carriers.

Table 1 gives an overview of the relevant technical details of the tested parts. The mean radius r_m and the nominal friction area A are used to calculate the CoF according to Eq. 1 and the utilized friction coefficient (UFC) according

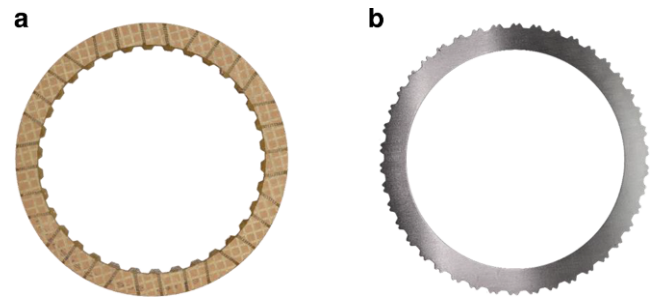


Fig. 1 Friction plate (a) and steel plate (b)

to Eq. 2. The nominal friction area A does not consider the groove pattern of the friction lining. The groove pattern is group-parallel multisegmented with a waffle imprint. The nominal clearance between each friction surface is set to be 0.2 mm.

The main goal of this study is the investigation of the influence of application-relevant surface finishes on the friction behavior of wet disk clutches. For this reason, the investigations consider three typical surface finishes. As a basis variant, we use steel plates with a polished and acid-etched finish from the serial application of a dual-clutch transmission (variant a). As variant b, a manufacturer of steel plates reworked steel plates of variant a with belt ground finish. Variant c is additionally brushed compared to variant b. Images made with the Alicona Infinite Focus G4 (see Fig. 7) in Fig. 2 show these surface finish variants with 50× magnification. According to the manufacturer, the hardness of the steel plates is between 280 and 325 HV10.

For the experiments, we use an application-relevant lubricant. The lubricant is a polyalphaolefin used in dual-clutch transmissions (DCT). Table 2 shows the physical properties of the lubricant available due to its safety data sheet.

Test rig KLP-260 (see Fig. 3) is a component test rig enabling the measurement of the dynamic friction behavior of whole clutches in different operation modes. A detailed explanation of the test rig, its technical data, and operation modes can be found in literature [38].

The outer carrier is connected to a load cell that provides the measurement of the friction torque T_f . Due to this design, the test rig operates in brake mode with a fixed outer carrier. The test rig allows several application relevant operation modes for automotive clutches. In brake shift operation, the main drive accelerates the inner shaft

Table 1 Technical details of the plates

Parameter	Unit	Value
Outer friction diameter d_a	mm	168.0
Inner friction diameter d_i	mm	141.0
Mean radius r_m	mm	77.3
Nominal friction area A	mm ²	6552.6

Fig. 2 Visual comparison of the investigated variants of steel plate surfaces before the run-in

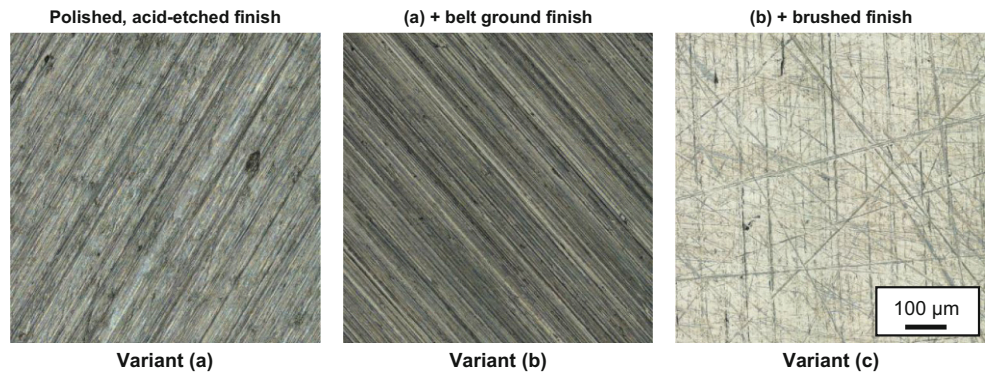


Table 2 Physical properties of the lubricant

Parameter	Unit	Value
Density @ 20 °C	kg/m ³	842
Kin. Viscosity @ 40 °C	mm ² /s	24.8
Kin. Viscosity @ 100 °C	mm ² /s	–

over a belt drive. When reaching a given speed, the main drive is disconnected from the inner shaft. After that, the axial force F_{ax} is applied by means of a hydraulic piston with integrated force and displacement measurement. The differential speed is reduced to standstill of the clutch. Another mode used for the investigations is forced unsteady operation. Here, the axial force F_{ax} is applied first. After that, the inner shaft is cyclically accelerated and decelerated five times (five slip phases) by a creep drive. Beside these modes, the test rig enables also other operation modes for the investigation of stationary slip and combinations of the shown modes in combination with different lubrication situations. In addition to the investigation of the friction behavior it also enables the investigation of the life time, damage and shudder behavior. The uncertainty of measurement for the test rig is discussed in detail in previous publications [13, 39, 40] and is dependent on the experimental dataset (e.g., axial force). For the shown measurements the

expanded relative measurement uncertainty for the CoF is between 1.4 and 2.0% (confidence level 95%).

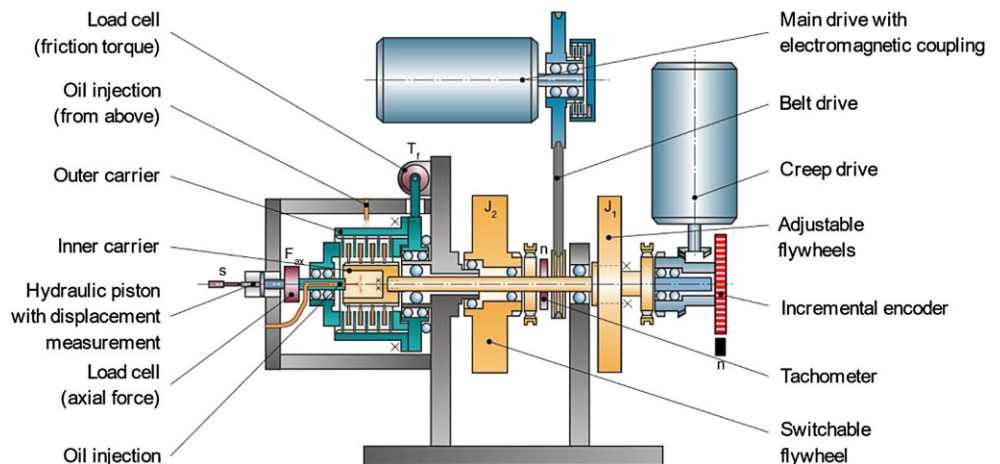
The clutch is lubricated half from the top and half from the inside with an overall specific oil flow rate of $0.8 \text{ mm}^3 \cdot (\text{mm}^2 \cdot \text{s})^{-1}$ with respect to the nominal friction area A .

In the publication, the measured course of the CoF according to Eq. 1 over the sliding speed v_g of the penultimate brake shift is evaluated and depicted.

$$\text{CoF} = \frac{T_f}{F_{ax} \cdot r_m \cdot z} = \frac{T_f}{p \cdot A \cdot r_m \cdot z} \tag{1}$$

In contrast to brake shift operation, the investigation of very low sliding speeds needs special treatment in evaluating the friction behavior. To minimize local effects at very low sliding speeds such as slightly slanted contact and thickness deviations of the plates, the course of the CoF over sliding speed is evaluated using its sliding average. These local effects have higher relevance in low speed slip due to the low number or even percentage of revolutions during an evaluated slip phase. Therefore, the CoF in the decelerating part of the third and fourth slip phase in cycles six to ten over slip speed is used to obtain a Characteristic Friction Curve (CFC). With this data, the sliding

Fig. 3 Schematic sketch of the component test rig KLP-260 according to Meingassner [38]



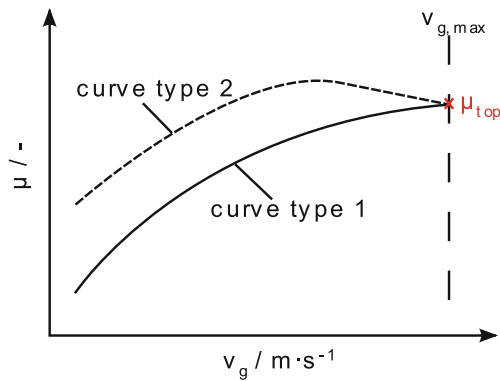


Fig. 4 μ_{top} for two types of friction characteristics with equivalent values of μ_{top} according to Strobl et al. [21]

average over slip speed is generated, which allows a stable comparison of different courses of the CoF over sliding speed. Evaluations only show small deviations between the individual curves. These are considered in the discussion of the influences in addition to the measurement uncertainty.

For parameter-based evaluations, the characteristic value μ_{top} according to Voelkel [31], is used to evaluate the CoF. Therefore, the CoF at maximum slip speed is determined. Fig. 4 shows the evaluation of μ_{top} at different curve types. Nevertheless, the friction behavior of the systems discussed here is continuously increasing (curve type 1). Here, μ_{top} is evaluated in the last slip phase of cycles six to ten.

On the other hand, component test rig LK-3 (Fig. 5) enables the measurement of the friction behavior at very low sliding speeds at the transition from static to dynamic friction. It can be used for the investigation of the creep behavior of wet disk clutches. As in KLP-260, the clutch is tested in brake mode with a fixed outer carrier. First, the clutch is loaded with a defined axial force F_{ax} via a screw. Then, torque is applied to the inner drive via a lever and weights. With this setup, different values of UFC are set, and the rotation of the lever is measured using a high precision incremental angle encoder and is recalculated to a sliding speed.

UFC is defined according to Voelkel et al. [12]. Here, the friction torque T_f is divided by the mean radius of the clutch

Fig. 5 Component test rig LK-3 according to Meingassner et al. [24]

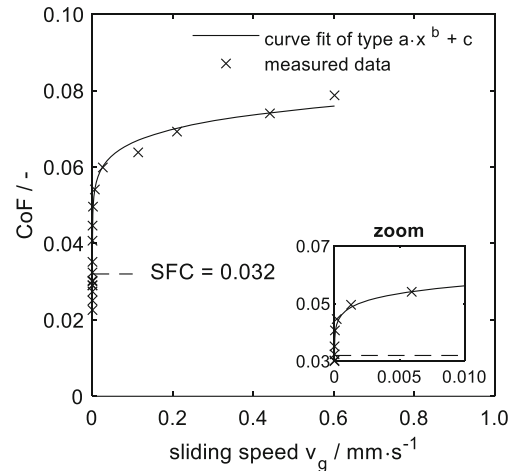
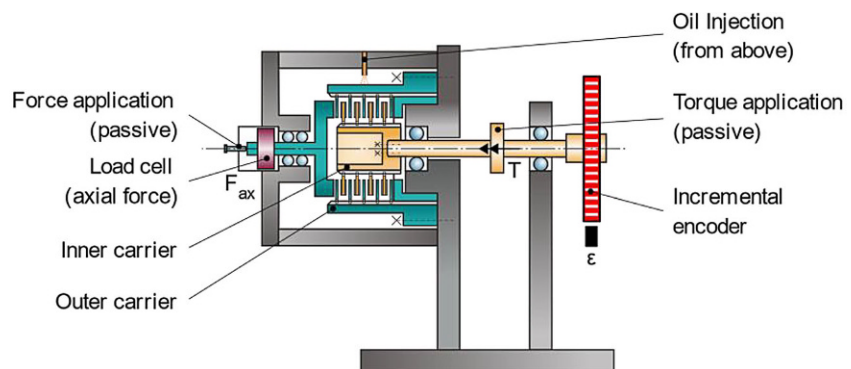


Fig. 6 Measured data, curve fit and SFC—exemplarily with measurements with steel plate variant (a) [$\vartheta_{\text{oil}} = 110^\circ\text{C}$; $p = 1.0 \text{N} \cdot \text{mm}^{-2}$]

r_m , the number of friction surfaces z , and the axial force F_{ax} . In this setup, the friction torque can also be calculated by the weight m , the gravitational acceleration g , the length l , and the current angle ϵ of the lever. The axial force can be written as the specific surface pressure p times the nominal friction area A . The uncertainty of measurement for the test rig is discussed in detail in previous publications [13, 39] and is dependent on the experimental dataset (e.g., axial force). For the shown measurements the expanded relative measurement uncertainty for the UFC is between 1.4 and 2.3% (confidence level 95%) [39].

$$\text{UFC} = \frac{m \cdot g \cdot l \cdot \cos(\epsilon)}{p \cdot A \cdot r_m \cdot z} \quad (2)$$

The evaluation of every single measurement leads to set of creep rate and corresponding UFC value. The measurements are repeated until no relevant creep rate can be observed within 10 to 15 min. At this point, the Static Friction Coefficient (SFC) is obtained. With all measurements showing creep a curve of type $f(v_g) = a \cdot x^b + c$ with ($0 < b < 1$) is fitted according to Voelkel et al. [12] to illustrate the creep behavior. Fig. 6 exemplarily shows data of the measurements and its corresponding curve fit as well as the

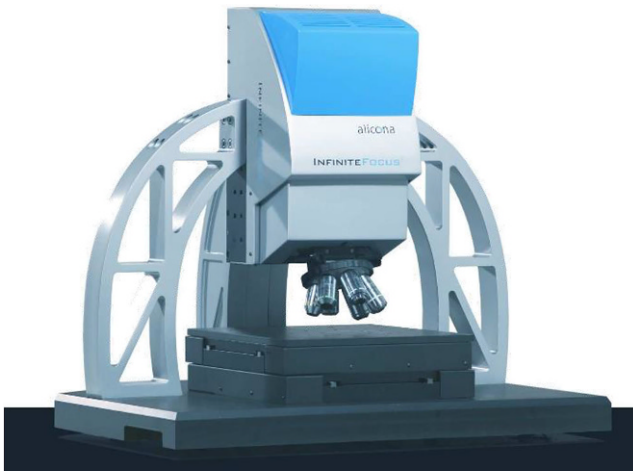


Fig. 7 Alicona Infinite Focus G4 [43]

Table 3 Settings for surface measurements

Parameter	Setting
Vertical resolution	50 nm
Lateral resolution	2 μ m
Measuring field	0.75 mm \times 0.75 mm
L-filter	250 μ m

Table 4 Description of surface parameters according to [37]

Parameter	Description
Sa	Arithmetical mean height
Sq	Root mean square height
Sp	Maximum peak height
Sv	Maximum pit depth
Sz	Maximum height
S10z	Ten-point-height
Ssk	Skewness
Sku	Kurtosis
Sdq	Root mean square gradient
Sdr	Developed interfacial area ratio
Sk	Core height
Spk	Reduced peak height
Svk	Reduced pit depth
Smr1	Material ratio of the hills
Smr2	Material ratio of the dales

determined SFC. Later, the curve fit is shown only at the transition of static and dynamic friction (see zoom). There is a detailed description of the methodology used to study wet disc clutches in creep behavior in literature [12–14].

In addition to the friction behavior, we measure the areal surface topography with the device Alicona Infinite Focus G4 shown in Fig. 7. This device works with the principle of focus variation, according to DIN EN ISO 25178-606 [41]. For the investigations, an objective with 50 \times magnification is used to resolve all necessary topography details. Table 3 provides the measuring settings for the determination of the areal roughness. The surface roughness is determined at eight evenly spaced circumferential positions for each side of one of the middle steel plates leading to a total of sixteen measurements representing the steel friction surface for each clutch. The measurement field is cut to a square of 0.75 \times 0.75 mm for each measuring position. This size guarantees a fast and reliable measurement of the surface topography with the usage of the objective with 50 \times magnification. To calculate roughness parameters in the measurement field, the shape is subtracted by alignment to a reference plane, and the waviness is subtracted by LC filtering with a Gaussian filter. The filter is set to be 250 μ m according to recommendations from profile measurements for values of Ra=0.02–0.1 in DIN EN ISO 4288 [42]. In pre-investigations, the resulting values Ra of the steel surfaces showed slightly higher values than 0.1. Taking into account the size of the measurement field and the resulting waviness, we decided to use the 250 μ m filter. The measurements presented guarantee a good comparison of the topography of different steel plate surfaces.

The roughness is determined in terms of standard areal surface parameters calculated according to DIN EN ISO 25178-2 [37]. Most of these areal parameters are derived from corresponding parameters of profile measurement, like arithmetical mean height Sa from Ra or core height Sk from Rk. In this paper, we investigate linear correlations between the friction behavior and 15 surface parameters. Table 4 gives an overview over the parameters. Further information on the definition of each of these parameters can be found in DIN EN ISO 25178-2 [37].

After explanation of the measurement setup, the following section describes the test procedure, including the test sequence, defined loads, and test conditions. Fig. 8 gives an overview of the test procedure. Variant (b) and (c) are tested with two clutches to evaluate the reproducibility of the tests. Due to a limited number of steel plates, variant (a) is only tested once. Nevertheless, clutches from serial production tend to show good reproducibility.

The clutches follow a run-in in brake shift operation to guarantee stable friction behavior in subsequent friction tests, according to Acuner et al. [44]. The load stages shown

Fig. 8 Test procedure

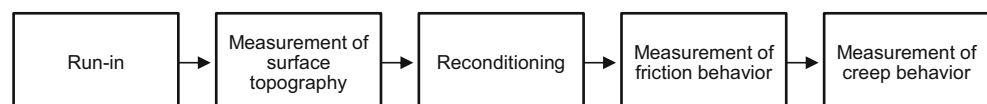


Table 5 Load stages in run-in / reconditioning according to Acuner et al. [44]

Name	$p / \text{N} \cdot \text{mm}^{-2}$	$V_{g,\text{max}} / \text{m} \cdot \text{s}^{-1}$	Cycles
RI1	0.5	6	100
RI2	0.5	12	100
RI3	1.0	12	200
RI4	1.0	18	200

Table 6 Load stages in brake shift operation

Name	$p / \text{N} \cdot \text{mm}^{-2}$	$V_{g,\text{max}} / \text{m} \cdot \text{s}^{-1}$	Cycles
BS1	0.5	10	10
BS2	0.75	10	10
BS3	1.0	10	10

Table 7 Load stages in unsteady slip operation

Name	$p / \text{N} \cdot \text{mm}^{-2}$	$V_{g,\text{max}} / \text{m} \cdot \text{s}^{-1}$	Cycles
US1	0.5	0.005	10
US2	0.75	0.005	10
US3	1.0	0.005	10
US4	0.5	0.01	10
US5	0.75	0.01	10
US6	1.0	0.01	10
US7	0.5	0.025	10
US8	0.75	0.025	10
US9	1.0	0.025	10
US10	0.5	0.05	10
US11	0.75	0.05	10
US12	1.0	0.05	10
US13	0.5	0.1	10
US14	0.75	0.1	10
US15	1.0	0.1	10
US16	0.5	0.2	10
US17	0.75	0.2	10
US18	1.0	0.2	10

in Table 5 are successively run through at an oil injection temperature of $\vartheta_{\text{oil}} = 80^\circ\text{C}$ and a connected inertia of around $1.1 \text{ kg} \cdot \text{m}^2$. The cycle time describing the time for the brake shift itself and the following cooling phase is set to be 15 s. In this period, the clutch is closed for 5 s before the open

cooling phase of 10 s starts, in which the inner shaft is accelerated up to the initial speed of the next brake shift.

After the run-in, the clutches are removed from the test rig to determine the topography of the surface at eight evenly distributed measuring positions along the mean friction radius according to the previously described measuring settings. For this reason, the friction surfaces are cleaned with a solvent to avoid any possible influence of lubricant artifacts on the optical surface measurement. Before resuming the investigation of the friction behavior, the clutches are reconditioned by thirty cycles of the run-in load stage RI4 at an oil injection temperature of $\vartheta_{\text{oil}} = 80^\circ\text{C}$.

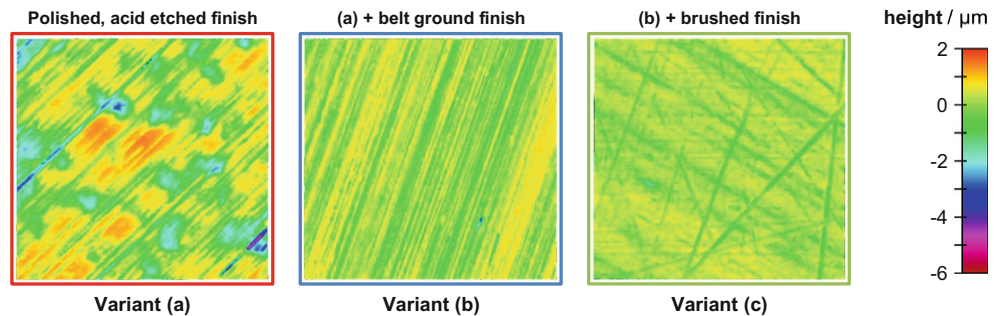
The investigations on the friction behavior are carried out in three blocks of different oil injection temperatures ϑ_{oil} ($80\text{--}110\text{--}40^\circ\text{C}$). Within each block, the friction systems are first tested in brake shift operation and after that, in unsteady slip mode. In the first step, ten brake shifts are performed in groups of ascending specific surface pressure p , see Table 6. Here, the cycle time is increased to 30 s compared to the run-in and conditioning to prevent the clutch from influences of the energy input of prior brake shifts.

In unsteady slip operation, ten cycles are performed with a total of eighteen combinations of sliding speed v_g and specific surface pressure p shown in Table 7. The load stages are performed with nominally increasing friction work to provide an appropriate prior load and are repeated in blocks of US1 to US18. The unsteady slip is determined based on five slip phases in each sequence, in which the clutch is accelerated in the closed state to a maximum differential speed within one second and then decelerated within one second again.

Due to restraints in the stable automated evaluation with very low sliding speeds, load stages US1–US3 were not considered in the following evaluations. The statements made later are not affected by these results.

After completion of the investigations at the KLP-260, the tested parts are installed in the LK-3 test rig and examined for their frictional behavior in micro slip and static friction. Before each test, the clutches are subjected to an axial force of 1000 N and forced to slide several times within an angular range of at least $\pm 15^\circ$. This guarantees a compa-

Fig. 9 Surface topography of the steel plates after the run-in



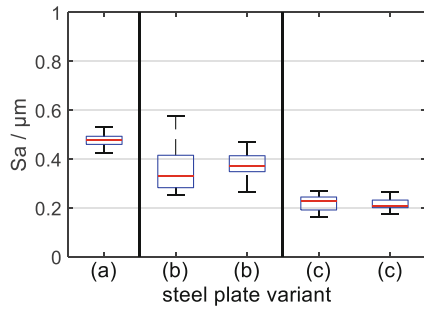


Fig. 10 Box-whisker plot of the arithmetic mean roughness Sa for each clutch

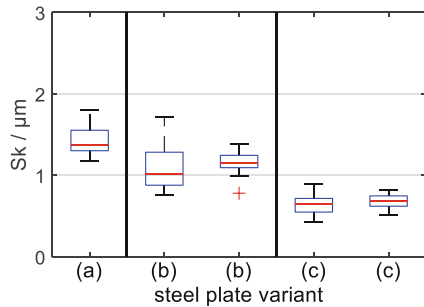
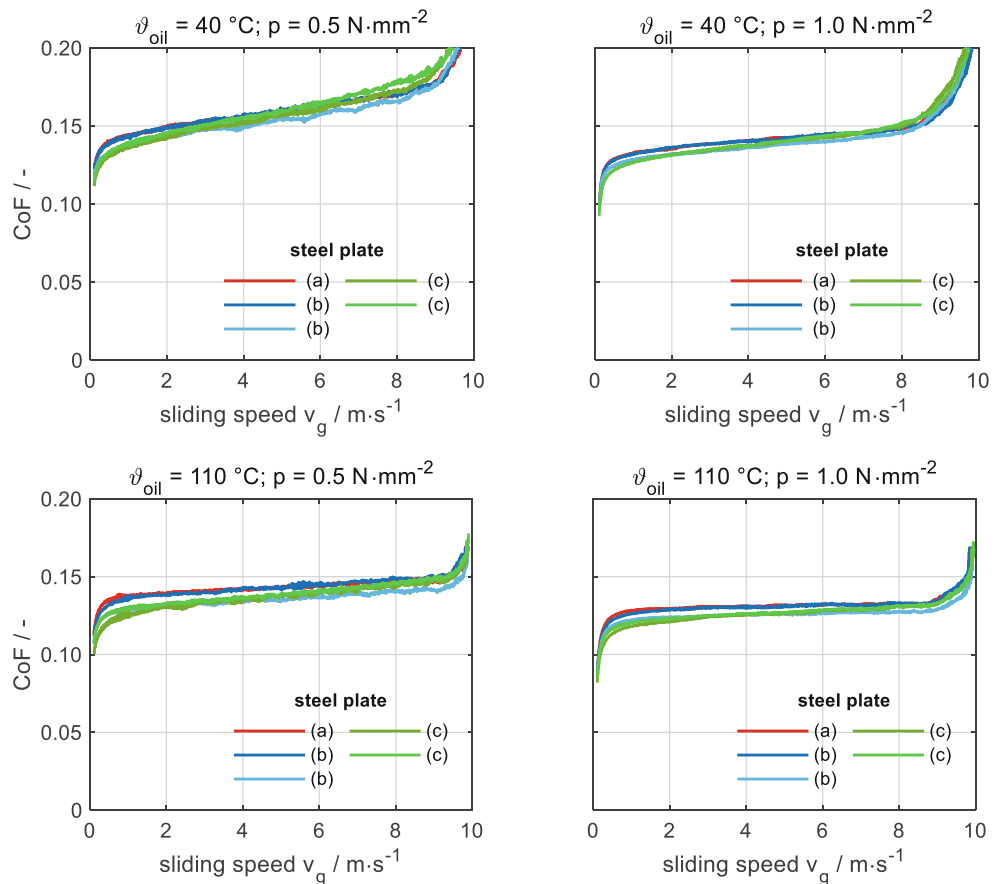


Fig. 11 Box-whisker plot of the core roughness Sk for each clutch

Fig. 12 Comparison of the friction behavior at brake shift operation of clutches with different steel plates at different operating conditions



erable preconditioning of the friction surfaces directly before the test and helps to reduce the influence of the preload. Due to high test runtimes, micro slip was investigated at two oil injection temperatures ϑ_{oil} (40 °C; 110 °C) and two specific surface pressures p (0.5 N · mm⁻²; 1.0 N · mm⁻²).

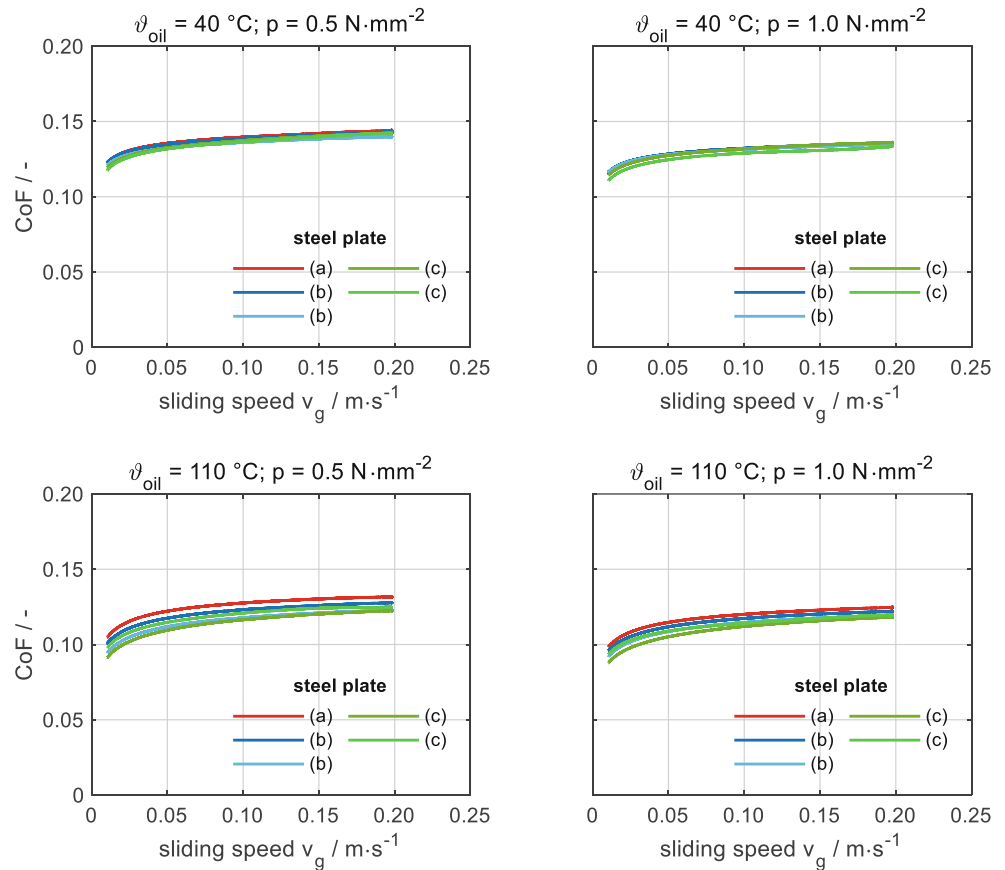
3 Results

3.1 Surface topography after run-in

Fig. 9 shows the surface topography of three exemplary sections of the investigated finishes by means of the height information after the run-in. The direction of sliding is horizontal in the image section. In the height information, smoothing in the direction of sliding is only slightly visible in variants (a) and (c) but not in variant (b).

Variant (a) shows a directional basic grinding structure overlaid by clustered elevation and depth ranges. Variant (b) only shows a directional grinding structure. Variant (c) shows a directional grinding structure overlaid by unidirectional patterns resulting from the additionally brushed finish. Due to the uniform choice of height scaling for all three measurements, it can already be visually recognized from the color scale that the roughness of the test

Fig. 13 Comparison of the friction behavior at unsteady slip operation of clutches with different steel plates at different operating conditions



parts decreases with each machining step. After running-in, the characteristic surface structures of all variants were retained. Structures in the sliding direction (horizontal) can be seen in a few areas in variant (a) and in many areas in variant (c) but not in variant (b).

This visual impression can also be quantified by areal topography parameters. For example, the mean arithmetic roughness S_a and the core height S_k are given in Fig. 10 and Fig. 11 for the tested clutches of different steel plate variants.

3.2 Friction behavior in brake shifts

First, the friction behavior in brake shifts is discussed. Fig. 12 shows the friction behavior in four parameter combinations of oil injection temperature ϑ_{oil} (top: 40 °C, bottom: 110 °C) and specific surface pressure p (left: 0.5 N·mm⁻², right: 1.0 N·mm⁻²) at brake shifts.

All brake shifts show a positive slope over the sliding speed. The high increase at the beginning of the brake shift (high sliding speeds) is caused by the axial force that builds up during engagement and is of no further interest. In general, there is a significant influence of the oil injection temperature and the specific surface pressure on the level and course of CoF.

Compared to these influences, the influence of the steel plate variant is to be considered minor. Nevertheless, it is noticeable and particularly evident in the comparison of variants (a) and (c). Variant (b) is difficult to classify between the two alternative steel plates. Particularly at low sliding speeds $< 2\text{ m}\cdot\text{s}^{-1}$, variant (c) shows a lower CoF than variant (a).

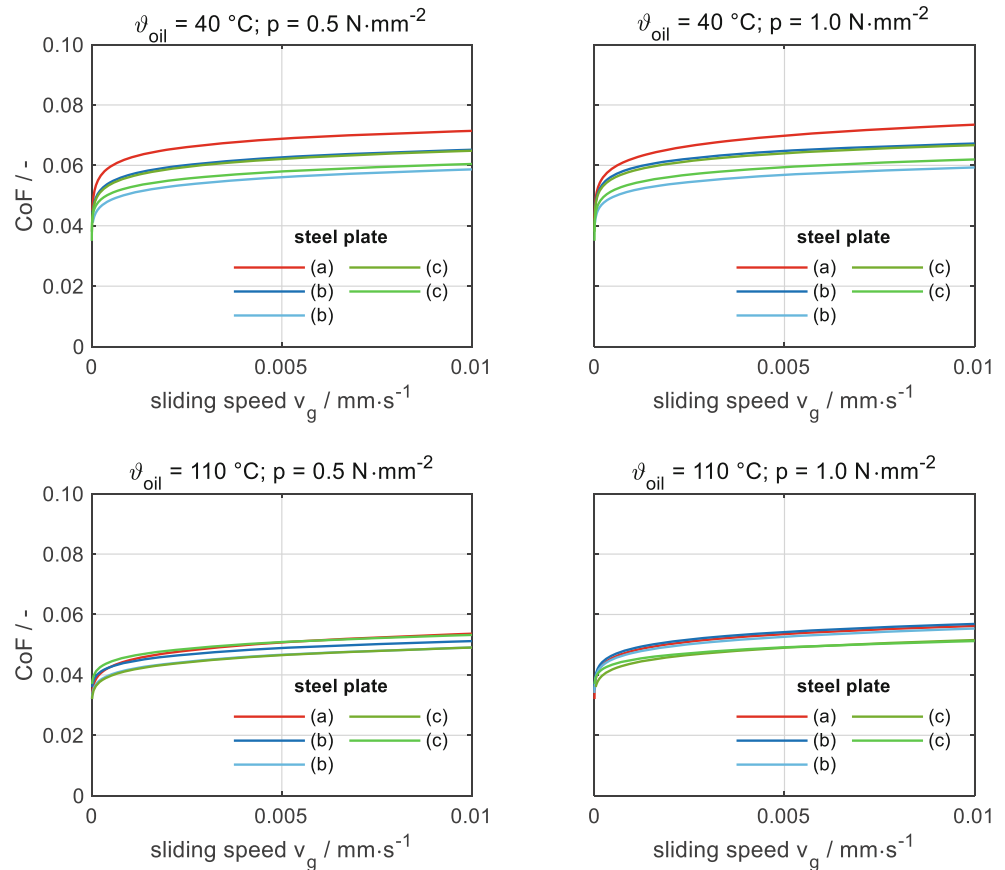
3.3 Friction behavior in unsteady slip

The influence at low sliding speeds can be observed in detail in the operation mode of unsteady slip. The friction behavior is discussed using the Characteristic Friction Curves (cfc) at four specific operating conditions with the maximum tested sliding speed ($v_{g,max} = 0.2\text{ m}\cdot\text{s}^{-1}$) in Fig. 13.

All CFC show a positive slope over the sliding speed in unsteady slip operation. A higher specific surface pressure p and a higher oil injection temperature ϑ_{oil} both lead to a reduction in the transmittable torque.

An influence of the steel plate variant on the friction behavior cannot be observed at an oil injection temperature of $\vartheta_{oil} = 40\text{ }^\circ\text{C}$. Thus, at the oil injection temperature of $\vartheta_{oil} = 110\text{ }^\circ\text{C}$, a reduction of the level of CoF can be seen at all specific surface pressures p . Here, variant (a) shows a higher level of CoF compared to variants (b) and (c).

Fig. 14 Comparison of the creep behavior of clutches with different steel plates at different operating conditions



Overall, variant (c) shows the lowest level of CoF, but the differences between variant (b) and variant (c) under consideration of all experiments are small.

3.4 Creep behavior and static friction

In addition to the investigations of the friction behavior at brake shifts and unsteady slip, creep behavior is investigated at the test rig LK-3 using a different test method.

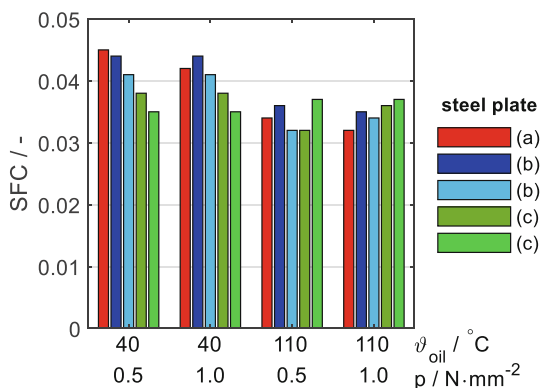


Fig. 15 Comparison of the SFC of clutches with different steel plates at different operating conditions

Fig. 14 shows the fitted curves of the creep behavior at sliding speeds of under 0.01 mm·s⁻¹. Here, the scaling of the CoF is adjusted compared to the previous figures to show differences in slip behavior better. In general, the level of the CoF is significantly lower than in unsteady slip and brake shift operations. Furthermore, the CoF has a steep gradient at very low sliding speeds.

The friction system with the steel plate variant (a) again tends to exhibit the highest friction coefficients—especially at an oil injection temperature of 40 °C—compared with the additionally reworked variants. However, it is not possible to clearly differentiate between variants (b) and (c) in terms of their creep behavior. Overall, both variants show a reduction in the coefficients of friction with higher oil injection temperatures. The influence of the specific surface pressure p on the creep behavior is subordinate.

This is also shown by the SFC determined at the transition between static and dynamic friction in Fig. 15. At an oil injection temperature of 40 °C, variant (a) shows the highest SFC. At an oil injection temperature of 110 °C, this cannot be observed.

3.5 Relation between CoF and surface topography in unsteady slip operation

In unsteady slip operation, we analyze the relation between CoF and surface parameters. Therefore, the median of the value μ_{top} of the fifth slip phase of cycles six to ten is determined for each clutch at every load stage. This representative friction coefficient value is compared to the median from the sixteen individual measurements of an areal surface topography parameter. Fifteen standard parameters are used to characterize the surface topography; see Table 4. In Fig. 16 and 17, the relation between CoF in unsteady slip operation and surface topography is shown for two standard surface parameters Sa and Sk at load stage US 18 ($p = 1.0 \text{ N} \cdot \text{mm}^{-2}$, $v_{g,max} = 0.2 \text{ m} \cdot \text{s}^{-1}$) at three oil injection temperatures. Both parameters indicate an influence of the surface topography parameter on the friction parameter μ_{top} at $\vartheta_{oil} = 80^\circ\text{C}$ and $\vartheta_{oil} = 110^\circ\text{C}$. Thus, no influence of these surface parameters on the friction behavior exists at $\vartheta_{oil} = 40^\circ\text{C}$. The linear curve fit is shown as a black line for each oil inlet temperature.

The coefficient of determination R^2 is determined for all investigated operating points in a combination of fifteen areal surface parameters. These values of R^2 are shown in Fig. 18. Here, values greater than 80% are highlighted dark green, values in the range of 60 to 79% are highlighted green and values in the range of 50 to 59% are highlighted yellow. This provides a visual impression of the goodness of fit for each surface parameter.

In this table, some surface parameters show high values of R^2 in combination with many operating conditions. Still, there are only few parameters showing a high coefficients of determination at an oil injection temperature of 110°C . Some parameters partly show very good correlation with many operating conditions especially at an oil injection temperature of 80°C . These are the arithmetical mean

height Sa, the root mean square height Sq, the maximum peak height Sp, the core height Sk, the reduced peak height Spk, and the reduced valley depth Svk.

4 Discussion

The tests in different operating modes show an influence of the steel plate surface on the friction behavior. The investigated steel plate variants show a change in the CoF level but no change in the friction behavior in the context of general gradient characteristics. In brake shift operation the influence of the steel plate surface tends to be observed more at the end of shifting when higher temperatures and lower sliding speeds are present in the clutch. This underlines the results in unsteady slip, where the influence of the steel plate variant is more likely to be detected at higher oil injection temperatures and, therefore, higher clutch temperatures. In creep behavior, the influence of the steel plate variant cannot be observed in all systems. Contrary to the unsteady slip operation where curves of CoF over sliding speed are generated using cfc evaluation, in micro slip, local effects at very low sliding speeds due to slightly slanted contact and thickness deviations of the plates are not minimized. Especially at sliding speeds that low, this might cause problems in interpreting variants with small differences in friction behavior.

Nevertheless, investigation of creep behavior and SFC show a similar behavior of all steel plate variants and support a better understanding of the overall friction behavior of wet disk clutches, where according to measurements of Meingassner [13], Meingassner et al. [14, 24] and Voelkel et al. [12] the SFC is significantly lower than the CoF at higher sliding speeds in unsteady slip or brake shift operation. This can be confirmed for the investigated clutches with different steel plate variants.

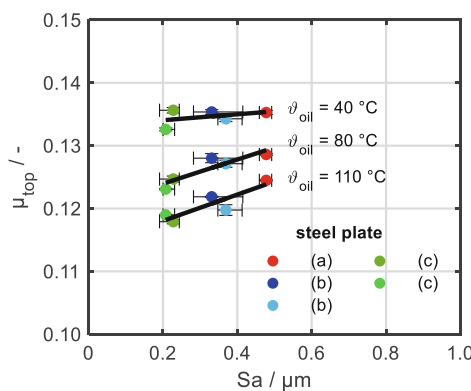


Fig. 16 Relation between the arithmetical mean height Sa and μ_{top} for different steel plate variants analyzed by linear regression (black) at three oil injection temperatures ϑ_{oil} in load stage US 18 ($p = 1.0 \text{ N} \cdot \text{mm}^{-2}$, $v_{g,max} = 0.2 \text{ m} \cdot \text{s}^{-1}$)

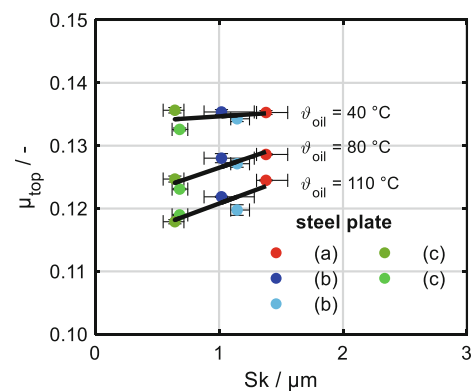


Fig. 17 Relation between the core height Sk and μ_{top} for different steel plate variants analyzed by linear regression (black) at three oil injection temperatures ϑ_{oil} in load stage US 18 ($p = 1.0 \text{ N} \cdot \text{mm}^{-2}$, $v_{g,max} = 0.2 \text{ m} \cdot \text{s}^{-1}$)

Fig. 18 Coefficient of Determination R^2 of the linear regression for every investigated combination of surface parameters and friction coefficient μ_{top} with highlighted high values of R^2

		R^2 of each combination load stage – surface parameter / %															
$\phi_{oil} / ^\circ C$	$p / N/mm^2$	$v_g / m/s$	Sa	Sq	Sp	Sv	Sz	S10z	Ssk	Sku	Sdq	Sdr	Sk	Spk	Svk	Smr1	Smr2
40	0.5	0.01	48	48	52	27	26	28	7	4	37	31	54	79	38	3	0
		0.025	48	51	65	50	50	52	1	2	63	57	54	93	56	6	0
		0.05	50	49	38	15	14	17	7	11	18	14	49	55	37	0	7
		0.1	5	4	0	6	6	4	40	52	2	5	3	11	0	0	8
	0.75	0.2	9	7	0	10	11	8	31	65	12	16	4	0	1	15	42
		0.01	77	79	91	72	71	73	3	4	74	68	85	82	80	0	0
		0.025	64	69	76	63	63	66	7	5	67	62	68	81	76	0	1
		0.05	63	65	44	29	30	35	7	0	23	20	55	33	65	10	32
	1.0	0.1	38	38	15	5	5	8	0	8	3	2	29	15	31	12	43
		0.2	24	23	3	0	0	0	4	26	1	2	16	4	13	19	54
		0.01	76	79	91	75	74	77	6	6	76	71	82	81	84	0	1
		0.025	55	61	71	70	72	75	25	19	71	69	58	68	79	0	2
80	0.5	0.05	63	69	65	62	64	69	29	15	55	53	61	47	84	3	12
		0.1	31	36	29	38	42	45	59	28	28	29	26	13	55	7	20
		0.2	17	19	6	5	6	9	21	1	2	2	10	2	25	16	46
		0.01	66	67	79	54	51	53	1	0	59	52	76	79	58	0	0
	0.75	0.025	78	79	86	60	57	60	0	0	61	54	87	74	70	0	0
		0.05	87	87	87	60	57	61	0	0	56	50	93	65	76	2	3
		0.1	84	84	81	53	50	54	0	0	51	45	88	68	73	2	4
		0.2	87	86	74	43	40	45	1	2	39	33	89	54	69	6	10
	1.0	0.01	67	68	84	62	59	61	0	1	68	61	77	84	64	1	0
		0.025	78	80	90	68	66	69	1	2	69	63	86	79	77	0	0
		0.05	83	85	89	64	62	66	1	1	63	57	89	74	80	1	2
		0.1	86	87	78	54	53	58	2	0	50	44	86	63	82	4	11
110	0.5	0.2	91	92	83	58	56	62	2	0	51	46	91	59	86	6	12
		0.01	67	69	86	65	62	64	0	1	71	64	78	84	65	1	1
		0.025	74	76	89	67	65	68	1	2	71	65	83	84	74	0	0
		0.05	83	85	92	73	71	75	4	4	71	66	88	76	86	0	2
	0.75	0.1	78	81	87	72	71	75	7	5	71	66	82	76	86	0	3
		0.2	82	86	79	64	64	69	12	5	56	52	81	56	91	5	13
		0.01	41	37	30	7	6	7	34	28	9	6	44	36	18	0	1
		0.025	42	38	29	6	5	6	34	30	8	5	44	35	18	1	2
	1.0	0.05	48	44	32	8	6	8	29	30	9	5	49	35	23	2	5
		0.1	52	48	34	9	7	10	25	27	10	6	52	37	27	3	7
		0.2	50	46	25	4	3	5	24	37	3	1	46	24	24	9	20
		0.01	33	30	26	5	4	5	39	29	8	5	37	37	13	0	0
0.75	0.025	44	39	32	8	6	8	32	27	10	6	47	37	20	1	2	
	0.05	51	47	35	9	7	9	27	27	10	6	52	36	25	3	5	
	0.1	50	46	34	9	7	9	26	27	10	7	51	39	26	2	5	
	0.2	57	52	29	6	5	7	20	32	5	2	52	25	29	11	21	
1.0	0.01	42	38	31	8	6	8	33	27	10	6	45	36	19	0	1	
	0.025	55	51	44	16	14	16	21	18	18	13	59	44	30	1	2	
	0.05	57	53	45	17	14	17	19	17	18	13	60	46	33	1	3	
	0.1	62	59	45	16	14	17	15	18	17	12	63	45	38	3	8	
0.2	78	75	56	25	23	27	5	10	22	17	76	44	54	8	16		

In all operation modes, an influence of the oil injection temperature on the friction behavior can be observed. Higher temperatures show a reduction of the CoF. Higher specific surface pressure also leads to a reduction of the CoF in all operation modes except in creep behavior, where no influence of the specific surface pressure on the friction behavior can be observed. Thus, in previous investigations, the specific surface pressure shows an influence on creep behavior as well [13].

A relation between oil injection temperature or viscosity behavior of the lubricant and the influence of the steel plate roughness on the friction behavior cannot be explained with the investigations since only one lubricant was used.

In further investigations, this could be a first approach to an improved understanding of the interaction between oil injection temperature, lubricant and friction surface. In addition, the topography of the lining friction surface should also be investigated and, if necessary, varied to determine interactions between the steel and friction lining surfaces. This would support a general understanding of an effect mechanism or formulation of a model conception as in the literature [2, 7], where the influence of different machinery settings for a specific surface finish on the friction behavior is investigated, and a first model conception is proposed.

Furthermore, several surface topography parameters can be determined, showing a good relation to the CoF in dif-

ferent load stages under unsteady slip conditions. These can be useful for quality control regarding this friction lining and lubricant combination. Higher values of those surface parameters after run-in show higher values of CoF which should be the aim for the development of friction systems. Areal surface parameters show good relations to CoF and low variance over several measurement positions over the steel plate, which also supports quality control due to a lower number of measurements, even though they might be more time-consuming to measure.

Due to the numerous interactions to be expected, the statements made are not directly transferable to friction systems with different friction linings or lubricants. The method presented here can be used to determine the influence of the steel plate finish on the friction behavior in various operation modes. The method can be adapted regarding the operating modes relevant for the corresponding application. An investigation of the relation between friction behavior and surface topography is proposed with the aid of areal characteristic values. A corresponding derivation of relevant surface characteristic values for internal as well as cross-company quality management can be defined based on the method for the respective friction system.

5 Conclusion

Steel plates with three different surface finishes are used to determine the influence of the surface topography of the steel plate on the friction behavior of wet disk clutches. The investigation shows a relation between the CoF and areal surface topography parameters for an application-relevant friction system with organic friction lining in unsteady slip operation. Other operation modes show similar tendencies.

The influence of the steel friction surface on the friction behavior is important for the optimization and design of wet disk clutch systems and should be considered in the design process as well as in quality control. Therefore, areal surface parameters are used due to their low variance and high informative value.

Acknowledgements The presented results are based on the research project FVA no. 343/V; self-financed by the Research Association for Drive Technology e. V. (FVA). The authors would like to express thanks for the sponsorship and support received from the FVA and the members of the project committee.

Funding Open Access funding enabled and organized by Projekt DEAL.

Open Access This article is licensed under a Creative Commons Attribution 4.0 International License, which permits use, sharing, adaptation, distribution and reproduction in any medium or format, as long as you give appropriate credit to the original author(s) and the source, provide a link to the Creative Commons licence, and indicate if changes were made. The images or other third party material in this article are

included in the article's Creative Commons licence, unless indicated otherwise in a credit line to the material. If material is not included in the article's Creative Commons licence and your intended use is not permitted by statutory regulation or exceeds the permitted use, you will need to obtain permission directly from the copyright holder. To view a copy of this licence, visit <http://creativecommons.org/licenses/by/4.0/>.

References

- Ito H, Fujimoto K, Eguchi M et al (1993) Friction characteristics of a paper-based facing for a wet clutch under a variety of sliding conditions. *Tribol Trans*. <https://doi.org/10.1080/10402009308983142>
- Bäse MU, Dzimko M, Deters L (2016) Empirische Bewertung von Zusammenhängen zwischen Endbearbeitungsparametern und Reibungsverhalten von Lamellenreibpaarungen im Mikroschlupfbetrieb. In: 57. Tribologie-Fachtagung, Aachen
- Ingram M, Noles J, Watts R et al (2010) Frictional properties of automatic transmission fluids: part I—measurement of friction-sliding speed behavior. *Tribol Trans*. <https://doi.org/10.1080/10402004.2010.531888>
- Ingram M, Noles J, Watts R et al (2010) Frictional properties of automatic transmission fluids: part II—Origins of friction-sliding speed behavior. *Tribol Trans*. <https://doi.org/10.1080/10402004.2010.531889>
- Ost W, de Baets P, Degrieck J (2001) The tribological behaviour of paper friction plates for wet clutch application investigated on SAE#II and pin-on-disk test rigs. *Wear*. [https://doi.org/10.1016/S0043-1648\(01\)00540-3](https://doi.org/10.1016/S0043-1648(01)00540-3)
- Mäki R, Nyman P, Olsson R et al (2005) Measurement and characterization of anti-shudder properties in wet clutch applications. SAE technical paper, vol 2005-01-0878. <https://doi.org/10.4271/2005-01-0878>
- Bäse MU (2016) Einfluss der Stahllamellen-Feinbearbeitung auf das Reibungsverhalten ölgeschmierter Lamellenreibkupplungen (PhD Thesis, Universität Magdeburg)
- Mäki R, Ganemi B, Höglund E et al (2007) Wet clutch transmission fluid for AWD differentials: influence of lubricant additives on friction characteristics. *Lubr Sci*. <https://doi.org/10.1002/lis.33>
- Mäki R, Ganemi B, Olsson R (2006) Wet clutch transmission fluid for AWD differentials: base fluid influence on friction characteristics. *Tribotest*. <https://doi.org/10.1002/tt.4>
- Marklund P, Mäki R, Larsson R et al (2007) Thermal influence on torque transfer of wet clutches in limited slip differential applications. *Tribol Int* 40:876–884. <https://doi.org/10.1016/j.triboint.2006.09.004>
- Marklund P, Larsson R (2007) Wet clutch under limited slip conditions—simplified testing and simulation. *Proc Inst Mech Eng Part J: J Eng Tribol* 221:545–551. <https://doi.org/10.1243/13506501JET252>
- Völkel K, Meingaßner GJ, Pflaum H et al (2021) Reibungsverhalten nasslaufender Lamellenkupplungen am Übergang Haftreibung – Gleitreibung. *Forsch Ingenieurwes*. <https://doi.org/10.1007/s10010-021-00437-2>
- Meingaßner GJ (2017) Methodik zur Untersuchung des Reibungsverhaltens nasslaufender Lamellenkupplungen bei Langsamlauf- und Mikroschlupf (PhD Thesis, Technische Universität München)
- Meingaßner GJ, Pflaum H, Stahl K (2017) Reibungsverhalten nasslaufender Lamellenkupplungen am Übergang Haftreibung – Gleitreibung. *VDI Berichte*, vol 2309, pp 159–172
- Groetsch D, Voelkel K, Pflaum H et al (2021) Real-time temperature calculation and temperature prediction of wet multi-plate clutches. *Forsch Ingenieurwes* 85:923–932. <https://doi.org/10.1007/s10010-021-00529-z>

16. Voelkel K, Wohlleber F, Pflaum H et al (2017) Kühlverhalten nasslaufender Lamellenkupplungen in neuen Anwendungen. VDI Berichte, vol 2309, pp 215–226
17. Wohlleber F (2012) Thermischer Haushalt nasslaufender Lamellenkupplungen (PhD Thesis, Technische Universität München)
18. Hämmerl B (1995) Lebensdauer- und Temperaturverhalten ölgekühlter Lamellenkupplungen bei Lastkollektivbeanspruchung (PhD Thesis, Technische Universität München)
19. Yang Y, Lam R, Fujii T (1998) Prediction of Torque Response During the Engagement of Wet Friction Clutch. SAE Technical Paper 981097. <https://doi.org/10.4271/981097>
20. Wang Y, Guo C, Li Y et al (2018) Modelling the influence of velocity on wet friction-element friction in clutches. *Ind Lubr Tribol* 70:42–50. <https://doi.org/10.1108/ILT-09-2016-0223>
21. Strobl P, Schermer E, Groetsch D et al (2022) Identification and validation of linear friction models using ANOVA and stepwise regression. *Lubricants* 10:286. <https://doi.org/10.3390/lubricants10110286>
22. Lloyd F, Reffett T, Wyatt D (1994) Static Friction – What It Is, What Affects It. SAE Technical Paper 941034. <https://doi.org/10.4271/941034>
23. Strobl P, Trapp M-L, Voelkel K et al (2023) Einfluss der Stillstandszeit auf das Reibungsverhalten nasslaufender Lamellenkupplungen im Übergang Haftreibung-Gleitreibung. *Tribol Schmierstech* 69(5–6):43–53. <https://doi.org/10.24053/TuS-2022-0044>
24. Meingaßner GJ, Pflaum H, Stahl K (2016) Drehmomentübertragungsverhalten nasslaufender Lamellenkupplungen bei geringen Differenzdrehzahlen. In: FVA (ed) GETLUB—Tribologie- und Schmierstoffkongress, Würzburg, pp 71–83
25. Albers A, Herbst D (1998) Chatter—causes and solutions. In: 6th LuK Colloquium
26. Albers A, Stier C (2011) Simulation von Anfahrvorgängen mit Kupplungsrupfen auf Basis experimentell ermittelter Antriebsstrang-Dämpfungseigenschaften. In: VDI (ed) Schwingungen in Antrieben 2011, pp 195–206
27. Layher M (2011) Einfluss der Schmierstoffadditivierung auf das Reibungsverhalten nasslaufender Reibschaltelemente (PhD Thesis, Technical University of Munich)
28. Farfan-Cabrera LI, Gallardo-Hernández EA, Vite-Torres M et al (2021) Influence of oxidation of automatic transmission fluids (ATFs) and sliding distance on friction coefficients of a wet clutch in the running-in stage. *Friction* 9:401–414. <https://doi.org/10.1007/s40544-020-0406-z>
29. Katsukawa M (2019) Effects of the physical properties of resins on friction performance. SAE technical paper, vol 2019-01-0341. <https://doi.org/10.4271/2019-01-0341>
30. Yagi S, Katayama N, Hasegawa H et al (2015) Effects of microscale texture on the tribological behavior of paper-based friction materials for a wet clutch. *Tribol Online* 10:390–396. <https://doi.org/10.2474/trol.10.390>
31. Voelkel K (2020) Charakterisierung des Einlaufverhaltens nasslaufender Lamellenkupplungen (PhD Thesis, Technical University of Munich)
32. Voelkel K, Pflaum H, Stahl K (2018) Running-in behavior of wet multi-plate clutches. In: FVA (ed) GETLUB International Conference, Hamburg, pp 1–7
33. Sittig K (2007) Tribologisch induzierte oberflächennahe Veränderungen der Stahl- und Belaglamellen einer nasslaufenden Lamellenkupplung (PhD Thesis, Universität Karlsruhe)
34. DIN Deutsches Institut für Normung e. V. (2022) Geometrical product specifications (GPS)—Surface texture: Profile—Part 2: Terms, definitions and surface texture parameters (DIN EN ISO 21920-2)
35. Geier N (2003) Untersuchung des Reibungs- und Verschleißverhaltens nasslaufender Kupplungen in Abhängigkeit ihrer Reibflächentopographie (PhD Thesis, Technical University of Munich)
36. Höhn B-R, Pflaum H, Geier N (2003) Kenngrößen zur Beurteilung der Oberflächentopographien von nasslaufenden Reibkupplungen. VDI Berichte, vol 1806, pp 115–125
37. DIN Deutsches Institut für Normung e. V. (2012) Geometrische Produktspezifikation (GPS) – Oberflächenbeschaffenheit: Flächenhaft – Teil 2: Begriffe und Oberflächen-Kenngrößen (DIN EN ISO 25178-2:2012-09)
38. Meingaßner GJ, Pflaum H, Stahl K (2015) Test-rig based evaluation of performance data of wet disk clutches. In: CTI (ed) 14th International CTI Symposium, Berlin
39. Hieber J (2022) Entwicklung eines ganzheitlichen Reibungszahlmodells für nasslaufende Lamellenkupplungen im Schlupfbetrieb (Master Thesis, Technical University of Munich)
40. Baumgartner A (2020) Reibungsverhalten nasslaufender Lamellenkupplungen – Messunsicherheiten und Auswertemethoden (Master Thesis, Technical University of Munich)
41. DIN Deutsches Institut für Normung e. V. (2016) Geometrische Produktspezifikation (GPS) – Oberflächenbeschaffenheit: Flächenhaft – Teil 606: Merkmale von berührungslos messenden Geräten (Fokusvariation) (DIN EN ISO 25178-606:2016-12)
42. DIN Deutsches Institut für Normung e. V. (1998) Geometrische Produktspezifikation (GPS) – Oberflächenbeschaffenheit: Tastschnittverfahren – Regeln und Verfahren für die Beurteilung der Oberflächenbeschaffenheit (DIN EN ISO 4288:1998-04)
43. Danzl R, Helml F, Rubert P et al (2008) Optical roughness measurements on specially designed roughness standards. In: Duparré A, Geyl R (eds) Optical Fabrication, Testing, and Metrology III. SPIE, 71020M
44. Acuner R, Pflaum H, Stahl K (2014) Friction screening test for wet multiple disc clutches with paper type friction material. In: Society of Tribologists and Lubrication Engineers Annual Meeting and Exhibition 2014. Society of Tribologists and Lubrication Engineers, Lake Buena Vista, pp 392–394